

Thin Bioactive Ceramic-Coated Alumina-Blasted/Acid-Etched Implant Surface Enhances Biomechanical Fixation of Implants: An Experimental Study in Dogs

Rodrigo Granato, DDS, MS;* Charles Marin, DDS, MS;† Jose N. Gil, DDS, MS, DSc;‡
Sung-Kiang Chuang, DMD, DMSc;§ Thomas B. Dodson, DMD, MPH;¶ Marcelo Suzuki, DDS;**
Paulo G. Coelho, DDS, MS, MSMtE, PhD††

ABSTRACT

Background: Thin bioceramic coatings have been regarded as potential substitutes for plasma-sprayed hydroxyapatite coatings.

Purpose: This study tested the hypothesis that a thin bioactive ceramic coating deposition on an alumina-blasted/acid-etched (AB/AE) surface would positively affect the biomechanical fixation and bone-to-implant contact (BIC) of plateau root form implants.

Materials and Methods: Implants of two different lengths (i.e., 4.5×11 mm long, $n = 36$) and 4.5×6 mm (short, $n = 36$) and two different surfaces, that is, control (AB/AE) and test (AB/AE + 300 – 500 nm bioactive ceramic coating), were placed in the proximal tibiae of six beagle dogs. The implants were retrieved for analyses 2 and 4 weeks after placement. The implants in bone specimens were subjected to torque loads until a 10% drop of the maximum torque was recorded. The specimens were evaluated under optical microscopy for bone morphology and percent BIC. Statistical analysis was performed by a generalized linear mixed effects analysis of variance model and statistical significance set at $p < 0.05$.

Results: Significantly higher torque-to-interface fracture levels for test surface groups of both lengths when compared to control surfaces were observed. No significant difference in BIC was observed between test and control implants of equal length. Histomorphological analysis showed higher degrees of bone organization between the plateaus of test implant surfaces at both implantation times.

Conclusion: Because the presence of a thin bioactive ceramic coating on the surface did not affect BIC, but positively affected implant biomechanical fixation, the hypothesis was partially validated.

KEY WORDS: bioactive ceramic, coating, dog, implant, in vivo, surface

*Research associate, School of Dentistry, Universidade Federal de Santa Catarina, Florianopolis, Brazil; †graduate student, School of Dentistry, Department of Oral and Maxillofacial Surgery, Pontificia Universidade Catolica do Rio Grande do Sul, Porto Alegre, Brazil; ‡assistant professor, School of Dentistry, Universidade Federal de Santa Catarina, Florianopolis, Brazil; §assistant professor, Department of Oral and Maxillofacial Surgery, Massachusetts General Hospital and the Harvard School of Dental Medicine, Boston, MA, USA; ¶associate professor, Department of Oral and Maxillofacial Surgery, Massachusetts General Hospital and the Harvard School of Dental Medicine, Boston, USA; **assistant professor, Department of Prosthodontics, Tufts University School of Dental Medicine, Boston, MA, USA; ††assistant professor, Department of Biomaterials and Biomimetics, New York University School of Dentistry, New York, NY, USA

Reprint requests: Dr. Paulo G. Coelho, 345 24th Street, Room 804s, New York, NY 10010, USA; e-mail: pgcoelho@nyu.edu

Because the implant surface is the first part of the implant that interacts with the host, increases in surface's biocompatibility and osseointegration have been attempted through a variety of engineering processes.^{1,2} Surface modification approaches have been successful in increasing the host response to surgical implants, resulting in higher bone-to-implant contact (BIC) and higher bone mechanical properties at early implantation times.¹⁻¹² Commonly utilized

© 2009 Wiley Periodicals, Inc.

DOI 10.1111/j.1708-8208.2009.00186.x

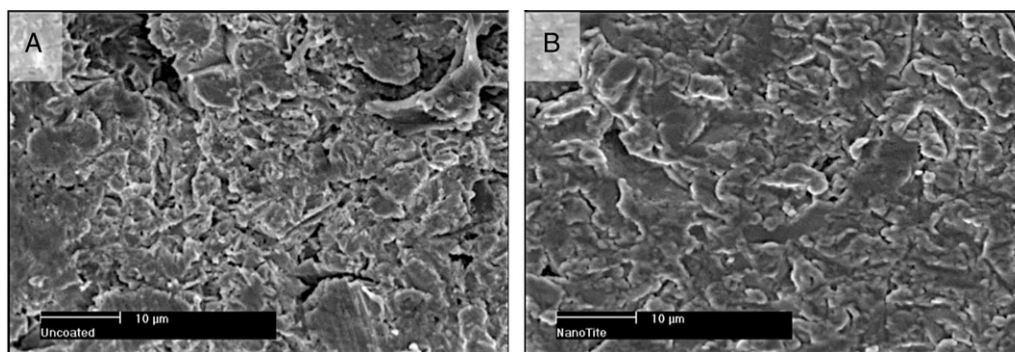


Figure 1 Scanning electron micrographs of (A) control and (B) test (right) surfaces. Note that at the scanning electron microscope (SEM) resolution, the 300–500 nm amorphous Ca- and P-based coating previously characterized by surface-specific analytical tools could not be depicted. At the SEM level, both surfaces presented similar morphology.

modifications that increase the biological response to implants are alterations in surface texture and alteration in surface chemistry such as the addition of calcium (Ca)- and phosphorous (P)-based bioceramic coatings to the implant surface.^{4,8,9,11,13}

Basic and clinical investigations have shown that bioceramic-coated, primarily plasma-sprayed hydroxyapatite (PSHA) implants presented higher degrees of osseointegration and attained higher degrees of biomechanical fixation at earlier implantation times compared to uncoated implants.^{6,9,11,13,14} However, studies have shown that because of their nonuniform thickness and composition, such coatings may be partially dissolved or resorbed after periods of *in vivo* function^{6,9,12,15} In addition, the interface between the bulk metal, metal oxide, and bioceramic coating has been regarded as a weak link, with adhesive failures.^{13,14}

In an attempt to benefit from the increased osseointegrative properties observed in calcium- and phosphate-based coatings while decreasing a long-term dependence on mechanical interlocking between coating and implantable device, smaller-scale bioceramic coatings have been developed for implant surfaces through various processing techniques.^{5,9–12} Some of these techniques are often applied in substantially thinner coating thicknesses (typically a few micrometers) compared to PSHA coatings.^{5,9,11} While promising results have been achieved through nanometer scale surface modifications,^{3,11–13,16–18} because of the different manufacturing processes and chemical/texture nuances between recently developed surfaces, the literature is sparse and contradictory, hindering further development of an informed design rationale for small thickness bioceramic coatings of endosseous implant surfaces.

The objective of this study was to evaluate the bone response (i.e., torque-to-interface failure and BIC) to a Ca- and P-based 300–500 nm thickness bioceramic deposition on a plateau root form Ti-6Al-4V implants in a dog model. The investigators hypothesize that higher degrees of biomechanical fixation and BIC would be observed for the thin-coated implants.

MATERIALS AND METHODS

This study utilized plateau root form endosseous Ti-6Al-4V implants (Bicon LLC, Boston, MA, USA) presenting two different surface treatments. The first type was an alumina-blasted/acid-etched (AB/AE) surface treatment (control; IntegraTi™, Bicon LLC, Boston, MA, USA), and the second comprised the ion beam-assisted deposition of an amorphous, high Ca-to-P ratio coating of 300–500 nm thickness (test; Nanotite™, Bicon LLC) over the AB/AE surface.¹⁹

All implants utilized presented 4.5 mm diameter, and half of the implants presented 11 mm in length (long, $n = 36$) and the other half 6 mm length (short, $n = 36$). An equal number of long and short implants presented control and test surface treatment. Scanning electron micrographs representative of each surface are presented in Figure 1. For mechanical testing purposes, an external hexagon was machined on the top of the implants for subsequent torque testing.

Following approval of the bioethics committee for animal experimentation at the Federal University of Santa Catarina, Florianopolis, Brazil, six male beagle dogs with ~1.5 years (ranging from 1 to 2 years of age) of age in good health were acquired for the study and remained in the facilities for a period of 1 month prior to surgery. The animals were born and raised in the

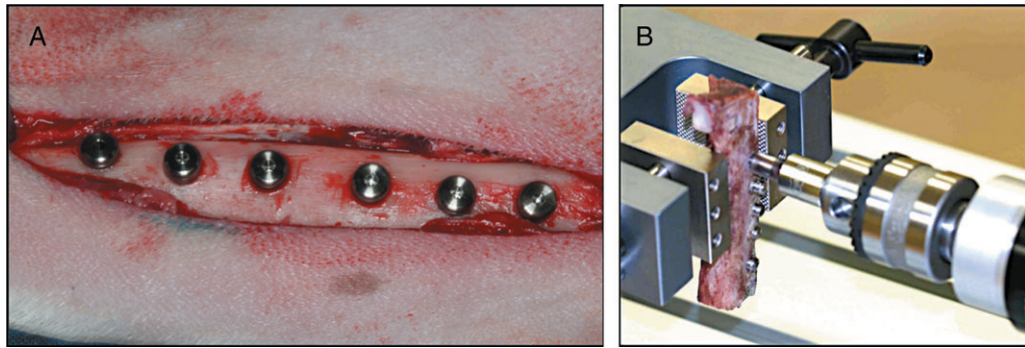


Figure 2 (A) Six implants were placed bilaterally along the beagle dog proximal tibia and were covered with healing caps. (B) Biomechanical torque testing setup showing specimen positioning in a grip avoiding rotation in the plane perpendicular to the long axis of the torque apparatus.

research animal facility at Universidade Federal de Santa Catarina.

The surgical region was the proximal tibia, and six implants were placed along each limb (12 implants per dog). Three animals were used for 2 and 4 weeks implantation time. The first implant was inserted 2 cm below the joint line at the central medial-lateral position of the proximal tibiae. The test and control implants were then alternately placed along the distal direction at distances of 1 cm from each other along the central region of the bone, and the starting implant length and surface was alternated between limbs and animals. The animals, limbs, and surgical site distributions for the 2- and 4-week comparison for test and control surfaces resulted in an equal number of implants per group (an equal number of implants were placed per surface, length, and time in vivo; $n = 9$). No randomization was performed.

All surgical procedures were performed under general anesthesia. The preanesthetic procedure comprised an intramuscular (IM) administration of atropine sulfate (0.044 mg/kg) and xylasin chlorate (8 mg/kg). General anesthesia was then obtained following an IM injection of ketamine chlorate (15 mg/kg).

Following skin exposure by means of a sharp blade and antiseptic cleaning with iodine solution at the surgical and surrounding area, a 5 cm incision at the skin level was performed and the subperiosteal dissection revealed the proximal tibia plateau. Six osteotomies were produced at least 10 mm from each other from proximal to distal. The initial drilling was performed by a 2 mm diameter pilot drill at 1,200 rpm under saline irrigation. Then, slow-speed (50 rpm, no saline irrigation) sequential drilling with burs of 2.5, 3.0, 3.5, 4.0, and 4.5 mm

diameter was performed. The implants were inserted using a press fit technique into the osteotomy sites.

In order to avoid any damage to the implant-bone interface because of removal of a callus overgrowth after limb retrieval, a customized cover screw was installed in each implant. Standard layered suture techniques were utilized for wound closure (4-0 vicryl-internal layers, 4-0 nylon; the skin). Postsurgical medication included antibiotics (penicillin, 20,000 UI/kg) and analgesics (ketoprophen, 1 mL/5 kg) for a period of 48 hours post-operatively. Euthanasia was performed by anesthesia overdose.

At necropsy, the upper third of the limbs were retrieved by sharp dissection, the soft tissue removed by surgical blades, and initial clinical evaluation was performed to determine implant stability.

All implants were subjected to torque-to-interface fracture. For biomechanical testing, the bone blocks with implants were adapted to an electronic torque machine equipped with a 2,000 Ncm torque load cell (Test Resources, Minneapolis, MN, USA). Customized machined tooling was adapted to the external hexagons, and each implant was carefully positioned to minimize specimen misalignment during testing (Figure 2). The implants were torqued to interfacial failure at a rate of ~ 0.196 rad/s, and a torque-versus-displacement curve was recorded for each specimen. The torque machine was set to automatically stop the measurement when a torque drop of 10% from the highest recorded torque was detected. The rationale for this procedure was to minimize interface damage prior to histological procedures, subsequently allowing BIC determination.¹⁹ As such, careful biomechanical testing allowed each block

to be used for both biomechanical and histological evaluation.¹⁹

Following biomechanical testing, the bone blocks were kept in 10% buffered formalin solution for 24 hours, washed in running water for 24 hours, and gradually dehydrated in a series of alcohol solutions ranging from 70 to 100% ethanol. Following dehydration, the samples were embedded in a methacrylate-based resin (Technovit® 9100, Heraeus Kulzer GmbH, Wehrheim, Germany) according to the manufacturer's instructions. The blocks were then cut into slices (~300 µm thickness) aiming the center of the implant along its long axis with a precision diamond saw (Isomet® 1000, Buehler, Düsseldorf, Germany), glued to acrylic plates with an acrylate-based cement (Aron Alpha® Industrial Crazy Glue, Elmer's Products, Inc., Columbus, OH, USA), and a 24-hour setting time was allowed prior to grinding and polishing. The sections were then reduced to a final thickness of ~30 µm by means of a series of SiC abrasive papers (400, 600, 800, 1,200, and 2,400) (Buehler) in a grinding/polishing machine (MetaServ® 3000, Buehler) under water irrigation.²⁰ The sections were then toluidine blue stained and referred to optical microscopy evaluation. The BIC was determined at 50 to 200× magnification (Leica DM4000, Wetzlar, Germany) by means of computer software (Leica Application Suite, Heerbrugg, Switzerland).

The primary predictor variable was implant surface (i.e., AE/AB vs AE/AB + ceramic coating). Secondary predictor variables were implant length (short and long) and duration in vivo (2 and 4 weeks). To address the research aim, the major predictor variable was the four groups of implants (implant length [short or long] and implant surfaces [control and test]). For statistical analyses, four groups were used and defined as short and control surface (used as reference), short and test surface, long and control surface, and long and test surface. To assess the adjusted relationship between various groups and the major outcomes (torque, BIC), the investigators constructed a generalized linear mixed effects analysis of variance (GLM ANOVA) model adjusting for multiple implants placed within the same animal ($n = 3$ animals per time in vivo). Level of statistical significance in the multivariate model was set at p values (an α level) of .05. All p values were two sided. Database preparation, management, and statistical analyses were carried out using SAS version 9.1 (2002–2003) statistical software (SAS Institute

Inc, Cary, NC, USA) using SAS procedure code proc mixed.

RESULTS

Histological Observations

Animal surgical procedures and follow-up demonstrated no complications regarding procedural conditions, post-operative infection, or other clinical concerns. During implant placement, both tibial cortices were included in the osteotomy of long implants, and only one was included for the short implants (Figure 3, A and B). Three implants were excluded from the study because of clinical instability immediately after specimen retrieval (implants failed to integrate), and another three were eliminated because of torque testing machine overshooting (still allowing BIC measurements, but torque values were not included in the statistical analysis).

The non-decalcified sample processing after torque testing showed direct bone contact along most of the implant surface at regions of cortical and trabecular bone for all groups (see Figure 3, C–F). Higher magnification of the bone-implant interface region showed that the non-decalcified sections obtained following biomechanical testing presented minimal morphological distortion caused by mechanical testing bone disruption. Under a magnification of 40×, the bone-implant interfaces were easily visualized and facilitated the BIC percentage determination (see Figure 3). No evidence of the thin-film bioceramic coating was observed in the histological sections because of the coating low thickness.

Appositional bone healing was observed at the plateau tips where direct contact existed between implant and bone immediately after placement. An intramembranous-like healing with rapid filling of the healing chamber formed between the implant plateaus by woven bone was observed.

Temporal morphological differences were observed for the different control and test group surfaces irrespective of implant length (see Figure 3, C and F). At 2 and 4 weeks implantation times, bone between test implants' plateaus presented qualitatively higher degrees of organization compared to the control group (see Figure 3, C–F). At 2 weeks, the presence of bone structural arrangements suggestive of lamella initial formation surrounding the rich blood vessel network was observed between test implants' plateaus (see Figure 3E), whereas the control implants presented diffuse woven bone

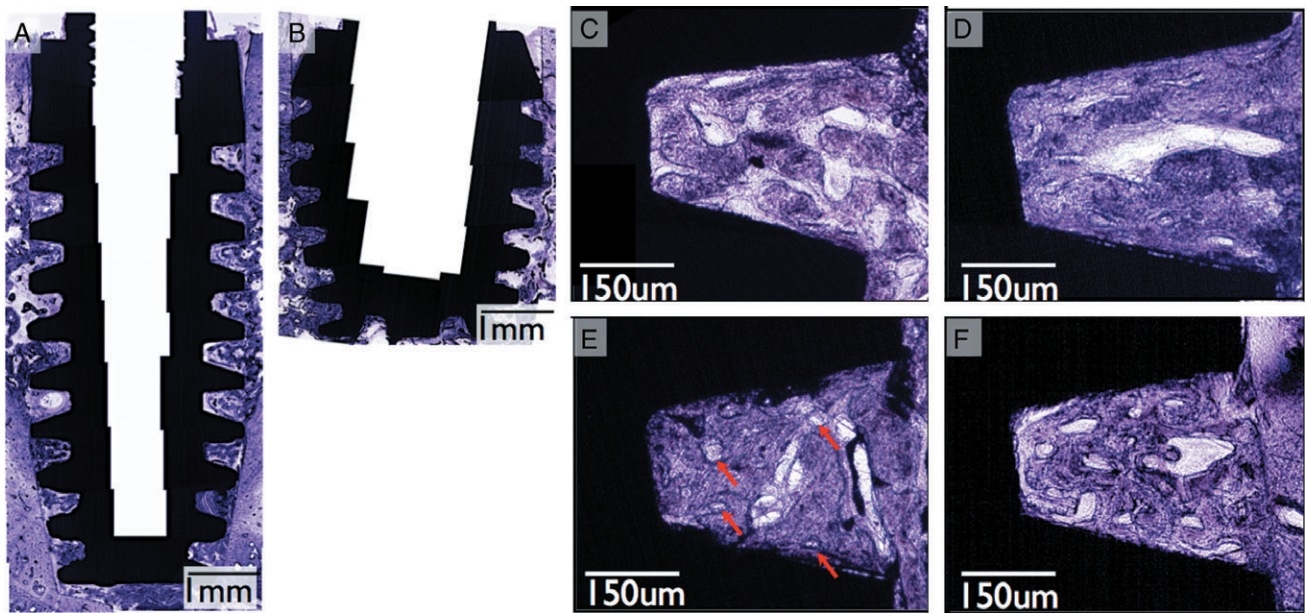


Figure 3 General histomorphology showing that (A) long implants were placed engaging both corticals, while (B) short implants engaged only one cortical. Histomorphological analysis between plateaus of different groups showed temporal differences as a function of control and test surfaces. At 2 weeks in vivo, the (C) control implant healing chamber was primarily filled with woven bone, while initial signs of modeling was observed for the (E) test surface (arrows). At 4 weeks, no substantial morphological evolution was observed for the (D) control surface compared to 2 weeks. However, lamellar bone regions surrounding an abundant vascular structure and marrow spaces were observed at various regions between the plateaus of (F) test implants at 4 weeks implantation time. (A and B original magnification 25 \times ; C–F original magnification 100 \times ; toluidine blue stain).

without organization indicative of modeling (see Figure 3C).

At 4 weeks implantation time, lamellar bone surrounding an abundant vascular structure, commensurate with primary osteonic structures, was observed at various regions between the plateaus of test implants (see Figure 3F), while no substantial evolution in bone morphology was apparent for the control implants at 4

weeks (see Figure 3D) compared to the 2 weeks implantation time.

Biomechanical Testing

The results of the GLM ANOVA for torque-to-interface fracture (Table 1) revealed that there were significantly higher torques for short test and long test implant groups when compared to the short control ($p = .0039$

TABLE 1 Analysis of Variance Table for Torque-to-Interface Fracture and Bone-to-Implant Contact (BIC)					
	Mean \pm SD	Coefficient	SE	t-Statistic	Pr > t
Test group (torque)					
Short test	57.33 \pm 25.87	30.82	10.24	3.01	0.0039
Long control	39.50 \pm 19.36	12.6	10.06	1.25	0.22
Long test	102.11 \pm 50.83	73.05	9.74	7.5	<0.0001
Short control (control and reference)	30.36 \pm 14.85	0 (Reference)	—	—	—
Test group (BIC)					
Short test	79.02 \pm 16.02	6.52	4.39	1.49	0.14
Long control	75.70 \pm 18.20	4.22	4.39	0.96	0.34
Long test	86.99 \pm 8.40	15.01	4.32	3.48	0.0009
Short control (control and reference)	71.70 \pm 20.37	0 (Reference)	—	—	—

Generalized linear mixed effects analysis of variance model adjusting for multiple implants placed within the same animal. Multivariate t -statistics were computed and p values were constructed.

and $<.0001$, respectively). In addition, there was no significant differences in torque between the long control and short control implant groups ($p = .22$).

Histomorphometry

For BIC, the results showed no statistically significant differences in BIC between the short test and long control compared to the short control implant group ($p = .14$ and $.34$, respectively). However, significantly higher BIC was observed for the long test group compared to the short control group ($p = .0009$, see Table 1). Time in vivo did not have a significant effect on torque-to-interface fracture and BIC.

DISCUSSION

This study aimed to investigate the effect of an ion beam-assisted deposition of an amorphous calcium and phosphorous based of 300–500 nm thickness onto a previously AB/AE implant substrate (test surface) on the biomechanical fixation, BIC, and bone morphology at early implantation times dog tibia model. The torque-to-interface fracture results showed that the test surface resulted in higher degrees of fixation at early implantation times, while comparable degrees of BIC were observed between control and test implant surfaces of the same length despite the qualitatively higher degrees of bone organization around test implant surfaces.

Because the definition of osseointegration as an intimate contact between bone and biomaterials occurring at the optical microscopy level,²¹ different approaches concerning device design have been employed attempting to increase the host-to-implant response. From a biomechanical perspective, bone-rough implant surface mechanical interlocking will generate higher biomechanical fixation results compared to smoother surfaces, and rougher surfaces are expected to present higher biomechanical fixation levels.^{1,2,22} However, previous work showed through nanoindentation that rougher surfaces resulted in higher bone mechanical properties compared to smoother surfaces at earlier implantation times.²³ Their results suggest that alterations in wound healing kinetics at early implantation times resulted from the implant surface roughness. From a surface roughness and texture perspective, previous analysis showed that the AB/AE surface presented average roughness (Ra) values ranging between 0.5 and 1 μm , and that the roughness profile was maintained

despite the thin coating deposition on test implant surfaces.¹⁹ Thus, despite differences in surface chemistry, both surfaces evaluated were moderately rough surfaces known to favor the host-to-implant response compared to as-turned surfaces.^{1,2}

Until recently, the only commercially available method where implant surface roughness and chemistry were substantially changed was by plasma spraying bio-compatible Ca- and P-based ceramics onto the implant surface, known as PSHA. However, concerns about inconsistent thicknesses and composition, and a potential weak link caused by the interface between coating and implant substrate^{8,18,24–27} has led to the production of coatings with substantially smaller dimensions compared to PSHA.

Previous in vitro and in vivo evaluations of bioceramic coatings of substantially thinner dimensions have shown promising results.^{10,11,18,27–28} However, the majority of investigations concerning reduced scale bioactive ceramic coatings evaluated implant design and surgical drilling which resulted in an intimate contact between the surface and bone immediately after surgery,^{10,11,27,29} resulting in a healing mode different than the intramembranous-like healing³⁰ observed for plateau root form implant utilized in the present study.

The biomechanical testing results in our experiment showed significantly higher torque-to-interface fracture for the test surface groups compared to control groups, revealing that the presence of the thin bioceramic coating on the implant surface positively influenced early host-to-implant response. Our results also showed that higher mean torque-to-interface fracture values were obtained for the short test implants compared to the long control implants despite the difference in length and available surface area for osseointegration. The high levels of torque-to-interface fracture for the test implants also suggest the absence of a weak link between bone, coating, and metallic substrate.^{12,18}

The experimental implant macrogeometry (no retentive features allowing free rotation in a plane) employed along with the torque-to-interface fracture methodology where proper alignment and precise loading until a 10% drop in the maximum torque was recorded was not detrimental to the subsequent histological measurements and interpretation.¹⁹ Thus, mechanical disruption was observed only in a few histological sections, and histomorphological evaluation and BIC determination were uneventful.¹⁹

Because the overall implant–bone system biomechanics is not only caused by BIC but also largely to the bone mechanical properties along and away the surface, and interaction at the bone-implant interface region, BIC measurements can only be used as an indicator of biocompatibility and osteoconductivity.^{8,19,31} In our study, the results showed no differences on BIC between test and control implants of similar dimensions. However, a significant difference was observed between the long test group versus the short control group. This result was likely related to differences in implant dimension where a monocortical osteotomy was drilled for the short implants versus a bicortical design utilized for the long implant placement.

The higher biomechanical fixation presented by the test implants with respect to control despite the same degrees of BIC is indicative of higher mechanical properties of the bone in proximity to the implant surface. However, studies involving the determination of bone mechanical properties around the different implants by means of micro- and nanoindentation²³ techniques are highly desirable to determine whether it is an interfacial phenomenon between bone and coating, or local and/or generalized increase in bone mechanical properties around test implants.

All sections evaluated throughout this study showed that the implants presented the majority of its bulk inserted into trabecular bone relative to cortical bone. General observation of the histological sections showed that the specimens from all groups demonstrated intimate bone contact to the implant irrespective of implant surface. Other findings include an agreement between the wound healing sequence and mode observed in our study, and the wound healing sequence described in detail by Berglundh and colleagues,³⁰ who showed that osseointegration establishment is relatively short for implants presenting large contact-free surfaces (healing chamber models). However, histomorphological evaluation showed higher degrees of bone organization for the test groups compared to the control group, which supports the biomechanical testing results where short and long test groups presented higher degrees of biomechanical fixation when compared to their control length counterparts, irrespective of the nonsignificant differences in BIC between groups of same implant length.

From a clinical standpoint, increased degrees of biomechanical fixation may potentially enable earlier loading of implants in a variety of clinical scenarios, including

the controversial treatment modalities such as early implant loading and posterior region treatment with short implants. While promising results concerning the early integration of thin-coated implants have been previously demonstrated and are further supported by our results, careful interpretation should be employed with respect to changes in treatment protocols. For that purpose, any alteration regarding a decrease in time frames between implant placement and loading must be rationalized and validated by prospective clinical trials.

CONCLUSION

This study investigated the hypothesis that higher degrees of biomechanical fixation and BIC would be observed for the thin-coated implants. Because the presence of a thin bioactive ceramic coating on the surface did not affect BIC but resulted in enhanced implant biomechanical fixation, the hypothesis was partially validated.

ACKNOWLEDGMENTS

This study was partially funded by Bicon LLC, Department of Oral and Maxillofacial Surgery at Federal University of Santa Catarina, and the Center for Applied Clinical Investigation, Department of Oral and Maxillofacial Surgery, Massachusetts General Hospital (S.-K.C. and T.B.D.).

REFERENCES

1. Albrektsson T, Wennerberg A. Oral implant surfaces: Part 1 – review focusing on topographic and chemical properties of different surfaces and in vivo responses to them. *Int J Prosthodont* 2004; 17:536–543.
2. Albrektsson T, Wennerberg A. Oral implant surfaces: Part 2 – review focusing on clinical knowledge of different surfaces. *Int J Prosthodont* 2004; 17:544–564.
3. Mendes VC, Moineddin R, Davies JE. The effect of discrete calcium phosphate nanocrystals on bone-bonding to titanium surfaces. *Biomaterials* 2007; 28:4748–4755.
4. Buser D, Broggini N, Wieland M, et al. Enhanced bone apposition to a chemically modified SLA titanium surface. *J Dent Res* 2004; 83:529–533.
5. Coelho PG, Lemons JE. IBAD nanothick bioceramic incorporation on metallic implants for bone healing enhancement. From physico/chemical characterization to in-vivo performance evaluation. Anaheim, CA: Nanoscience and Technology Institute, 2005.
6. deGroot KKC, Wolke JGC, deBieck-Hogervorst JM. Plasma-sprayed coating of calcium phosphate. In: Yamamuro THL, Wilson J, eds. *Handbook of bioactive ceramics*, Vol. II.

- Calcium phosphate and Hydroxyapatite ceramics. Boca Raton, FL: CRC Press, 1990:17–25.
7. Klokkevold PR, Nishimura RD, Adachi M, Caputo A. Osseointegration enhanced by chemical etching of the titanium surface. A torque removal study in the rabbit. *Clin Oral Implants Res* 1997; 8:442–447.
 8. Lemons JE. Biomaterials, biomechanics, tissue healing, and immediate-function dental implants. *J Oral Implantol* 2004; 30:318–324.
 9. Ong JL, Carnes DL, Bessho K. Evaluation of titanium plasma-sprayed and plasma-sprayed hydroxyapatite implants in vivo. *Biomaterials* 2004; 25:4601–4606.
 10. Orsini G, Piatelli M, Scarano A, et al. Randomized, controlled histologic and histomorphometric evaluation of implants with nanometer-scale calcium phosphate added to the dual acid-etched surface in the human posterior maxilla. *J Periodontol* 2006; 77:1984–1990.
 11. Park YS, Yi KY, Lee IS, Han CH, Jung YC. The effects of ion beam-assisted deposition of hydroxyapatite on the grit-blasted surface of endosseous implants in rabbit tibiae. *Int J Oral Maxillofac Implants* 2005; 20:31–38.
 12. Kim HS, Yang Y, Koh JT, et al. Fabrication and characterization of functionally graded nano-micro porous titanium surface by anodizing. *J Biomed Mater Res B Appl Biomater* 2008; 88(2):427–435.
 13. Catledge SA, Fries MD, Vohra YK, et al. Nanostructured ceramics for biomedical implants. *J Nanosci Nanotechnol* 2002; 2:293–312.
 14. Kay J. Calcium phosphate coatings for dental implants. *Dental Clin North Am* 1992; 36:1–18.
 15. Lemons J, Dietch-Misch F. Biomaterials for dental implants. In: Misch CE, ed. *Contemporary implant dentistry*. Saint Louis, MO: Mosby, 1999:271–302.
 16. Coelho PG, Suzuki M. Evaluation of an IBAD thin-film process as an alternative method for surface incorporation of bioceramics on dental implants. A study in dogs. *J Appl Oral Sci* 2005; 13:87–92.
 17. Coelho PG, Freire JNO, Coelho AL, et al. Bioceramic coatings: improving the host response to surgical implants. In: Liepsch D, ed. *5th World Congress of Biomechanics, 2006, Munich, Germany*. Munich: Medimont, 2006:253–258.
 18. Ong JL, Bessho K, Carnes DL. Bone response to plasma-sprayed hydroxyapatite and radiofrequency-sputtered calcium phosphate implants in vivo. *Int J Oral Maxillofac Implants* 2002; 17:581–586.
 19. Coelho PG, Lemons JE. Physico/chemical characterization and in vivo evaluation of nanothickness bioceramic depositions on alumina-blasted/acid-etched Ti-6Al-4V implant surfaces. *J Biomed Mater Res A* 2008. (In press)
 20. Donath K, Breuner G. A method for the study of undecalcified bones and teeth with attached soft tissues. The Sage-Schliff (sawing and grinding) technique. *J Oral Pathol* 1982; 11:318–326.
 21. Branemark PI, Adell R, Breine U, Hansson BO, Lindstrom J, Ohlsson A. Intra-osseous anchorage of dental prostheses. I. Experimental studies. *Scand J Plast Reconstr Surg* 1969; 3:81–100.
 22. Albrektsson T, Branemark PI, Hansson HA, Lindstrom J. Osseointegrated titanium implants. Requirements for ensuring a long-lasting, direct bone-to-implant anchorage in man. *Acta Orthop Scand* 1981; 52:155–170.
 23. Butz F, Aita H, Wang CJ, Ogawa T. Harder and stiffer bone osseointegrated to roughened titanium. *J Dent Res* 2006; 85:560–565.
 24. Lacefield WR. Hydroxyapatite coatings. *Ann N Y Acad Sci* 1988; 523:72–80.
 25. Lacefield WR. Current status of ceramic coatings for dental implants. *Implant Dent* 1998; 7:315–322.
 26. LeGeros RZ. Properties of osteoconductive biomaterials: calcium phosphates. *Clin Orthop Relat Res* 2002; 395:81–98.
 27. Yang Y, Kim KH, Ong JL. A review on calcium phosphate coatings produced using a sputtering process – an alternative to plasma spraying. *Biomaterials* 2005; 26:327–337.
 28. Coelho PG, Suzuki M. Evaluation of an IBAD thin-film process as an alternative method for surface incorporation of bioceramics on dental implants. A study in dogs. *J Appl Oral Sci* 2005; 13:87–92.
 29. Mendes VC, Moineddin R, Davies JE. Discrete calcium phosphate nanocrystalline deposition enhances osteoconduction on titanium-based implant surfaces. *J Biomed Mater Res A* 2008. (Epub ahead of print)
 30. Berglundh T, Abrahamsson I, Lang NP, Lindhe J. De novo alveolar bone formation adjacent to endosseous implants. *Clin Oral Implants Res* 2003; 14:251–262.
 31. Coelho PG, Granjeiro JM, Romanos GE, et al. Basic research methods and current trends of dental implant surfaces. *J Biomed Mater Res B Appl Biomater* 2009; 88(2):579–596.

Copyright of Clinical Implant Dentistry & Related Research is the property of Wiley-Blackwell and its content may not be copied or emailed to multiple sites or posted to a listserv without the copyright holder's express written permission. However, users may print, download, or email articles for individual use.